Analysis of Globus-M2 tokamak plasma heating experiments using diamagnetic measurements

E.E. Tkachenko[1,2], N.V. Sakharov[1], G.S. Kurskiev[1], N.S. Zhiltsov[1], I.V. Miroshnikov[1], Yu.V. Petrov[1], V.B. Minaev[1], N.N. Bakharev[1], A.A. Kavin[3] , E.O. Kiselev[1], K.M. Lobanov[3], A.N. Novokhatskii[1], A.B. Mineev[3], V.V. Solokha[1], E.A. Tukhmeneva[1], N.A. Khromov[1].

[1]*Ioffe Institute, St. Petersburg 194021, Russia*
[2]*Peter the Great St. Petersburg Polytechnic University, St. Petersburg, Russia*
[3]*JSC «NIIEFA», St. Petersburg, Russia*

IOTW 2022
The 21st International Spherical Torus Workshop

Introduction

- The evolution of plasma thermal energy was estimated using the free boundary equilibrium code PET. The code solves the Grad–Shafranov equation and also calculates the magnetic flux measured with the diamagnetic loop.
- The last closed magnetic surface was reconstructed by the method of movable filaments.
- Last closed magnetic surface and diamagnetic flux were used as fitting parameters for PET simulation. Such approach made it possible to determine the plasma thermal energy as well as the normalized internal inductance.
- Total plasma thermal energy and internal inductance were compared with approximate equations.

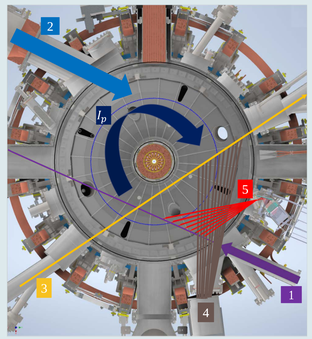

Fig 1. Globus-M2 scheme. 1 – first neutral beam injector (NBI^1); 2 - second neutral beam injector (NBI^2); Tomson scattering diagnostic: 3 – laser injection line; 4 – sightlines; 5 – sightlines of CXRS.

Globus-M2 spherical tokamak	
R, m	0,36
a, m	0,24
R/a	1,5
Elongation	2
Triangularity	≤0,4
B_{tor}, T	0.9
I_p, MA	0,3-0,4
P_{OH}, MWt	0,35
E^1_{NBI}, keV	28
E^2_{NBI}, keV	40-47
P_{NBI}, MWt	1,2-1,4

Diagnostics

Tomson scattering diagnostic provides accurate local electron temperature T_e and density n_e measurements. Nd:YAG laser with a wavelength of 1064 nm and a pulse repetition rate of 330 Hz is used in diagnostic [1]. Measurements are performed for ten spatial points from the magnetic axis to the last closed magnetic surface on the low magnetic field side and at one spatial point on the other side of the axis.

Charge exchange recombination spectroscopy (CXRS) [2,3] provide measurement of ion temperature profile. The CXRS diagnostics system consists of a specially developed optics with eight observation «chords» to collect the light signal. The system time resolution is 5 ms.

Instruments

Equilibrium code PET

- Free boundary FORTRAN code [4].
- PET solves the Grad–Shafranov equation by using approximations

$$\frac{dP}{d\Psi_p} = \alpha_0\left[1-\left(1-\Psi_p(r)\right)^{\alpha_1}\right]^{\alpha_2}$$

$$I_p\frac{dI_p}{d\Psi_p} = \alpha_0\left[1-\left(1-\Psi_p(r)\right)^{\alpha_1}\right]^{\alpha_2}$$

- PET calculates the magnetic flux measured with the diamagnetic loop
- In PET simulation the shapes of plasma pressure and current density profiles, as well as plasma beta (β_l) were varied. The last closed magnetic surface reconstructed by the movable filaments method and the diamagnetic flux were used as fitting parameters
- This approach made it possible to determine the plasma thermal energy W_p as well as the normalized internal inductance l_i and volume averaged parameters.

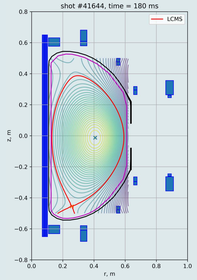

Fig. 2. Geometry of PET-code. Blue rectangular is a poloidal field coils, red line is the last closed magnetic surface.

$$\beta_l = \frac{8\pi\int pdS}{\mu_0 I_p^2} \qquad l_i = \frac{2V<B_p^2>}{(\mu_0 I_p)^2 R}$$

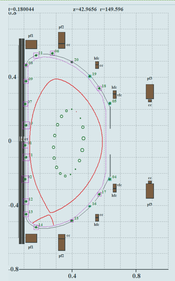

Fig. 3. Geometry of the method of movable filaments.

The method of movable filaments

- The method provides reconstruction of last closed magnetic surface.
- In this method [5] the plasma current is modeled by a set of 19 current-carrying rings. The input data are the magnetic fluxes measured by 21 loops placed on the vacuum vessel wall near the plasma boundary, the plasma current and the currents in PF coils and central solenoid
- The signals from the magnetic loops were also used to determine the distribution of the currents over the vessel wall

Results

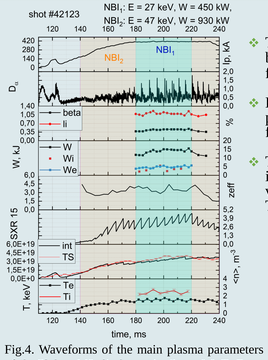

Fig.4. Waveforms of the main plasma parameters of theGlobus-M2 discharge in B_T = 0.9 T. From top to bottom: plasma current; Dα emission intensity; β_l (black) and l_i (red); plasma energy: black—total plasma energy by PET, blue — thermal energy of electrons from the TS, red - thermal energy of ions from the CXRS; effective charge from intensity of bremsstrahlung; intensity of soft-x-ray emission with 15 mkm foil; volume average density: black line—interferometer, red line—TS; temperature in the plasma center: black line - electron temperature measured by TS, red line — ion temperature by CXRS.

- The stored energy of plasma in discharges with two beams, $B_T = 0.9$ T field and $I_p = 400$ kA current as a function of electron density was analyzed (fig,5).
- Hydrogen beams were injected into the deuterium plasma. The parameters of the beams are shown in the fig.5 for each group of discharges.
- The stored energy in electrons was obtained by integration of pressure profiles over the entire plasma volume. The pressure profiles were obtained using Thomson scattering diagnostic.

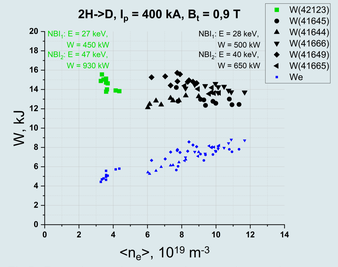

Fig.5. Dependence plasma stored energy from volume average density. Black and green dot – total plasma energy by PET, blue dot - thermal energy of electrons from the TS and PET.

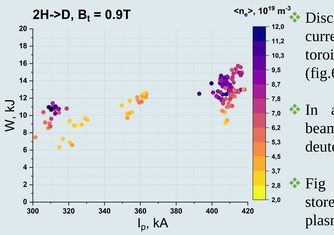

Fig.6 Dependence total plasma energy from plasma current.

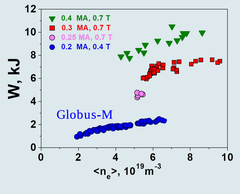

Fig.7 Plasma stored energy vs density for different I_p and B_T.

- Discharges with different plasma currents (300-400 kA) and 0.9T toroidal field were analyzed (fig.6).
- In all discharges, 2 hydrogen beams were injected into the deuterium plasma.
- Fig 6 shows that total plasma stored energy increased with plasma current ascension.
- In previous work [6] (fig. 7) it has been shown that at a field up to 0.8 T and a single beam of neutral injection, the maximum value of W_{approx} was up to 10 kJ. This means that in experiments with two NBI and $B_T = 0{,}9T$ plasma stored energy is 1,5 times larger.
- On Globus-M [7], the maximum W_{approx} reached 3 kJ at the average electron density $6 \cdot 10^{19}\ m^{-3}$ and $B_T = 0.4T$, $I_p = 200\ kA$.

Comparison with approximate equations

- Measuring the diamagnetic flux from the plasma allows us to calculate the diamagnetic beta β_{dia}[8]:

$$\beta_{dia} = 1 + \frac{\kappa^2+1}{2\kappa}\frac{B_t\Psi_{\text{dia}}}{20\pi I_p^2}$$

- The mathematical model of Globus-M2 made it possible to determine the vertical magnetic field B_v. Then it is possible to determine l_i using the β_{dia} as the β_p.

$$B_v = \frac{\mu_0 I_p}{4\pi R}\left(ln\frac{8R}{a\kappa^{\frac{1}{2}}} - \frac{3}{2} + \beta_p + \frac{l_i}{2}\right)$$

- Using the definition of beta, we can define the stored plasma energy through the following approximate formula:

$$W_{approx} = \frac{3}{2}\frac{\beta_{dia}\,\mu_0 I_p^2 R}{4}$$

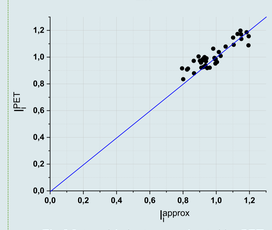

Fig.8 Internal inductance estimated by PET vs internal inductance obtained by the approximate equation.

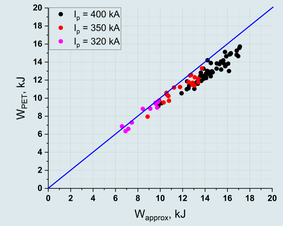

Fig.9 Total stored plasma energy estimated by PET vs diamagnetic total plasma energy.

Conclusion

- The experiments on heating the plasma of the Globus-M2 tokamak by two beams of neutral injection were analyzed. The interpretation of the diamagnetic measurements by the equilibrium code PET was used for the analysis.
- In this work, it has been shown that plasma storage energy increases with an increase in average electron concentration, plasma current, and heating beam power.
- The total plasma energy in experiments with two heating beams and a 0.9T magnetic field is 1.5 times higher than the plasma storage energy obtained with one heating beam and a 0.8T magnetic field.
- Compared to Globus-M ($B_T = 0.4T$, $I_p = 200\ kA$) total plasma stored energy increased 5 times.

References

[1] Kurskiev G.S. et al 2021 *Tech. Phys. Lett.* 47 41
[2] Avdeeva G.F., Miroshnikov I.V., Bakharev N.N., Kurskiev G.S., Patrov M.I., Sergeev V.Y. and Schegolev P.B. 2016 *J. Phys.: Conf. Ser.* 666 012002
[3] Larionova M.M. et al 2019 *J. Phys.: Conf. Ser.* 1400 077018
[4] S.A. Galkin, A.A. Ivanov, S.Yu. Medvedev and Yu.Yu. Poshekhonov, *Nucl. Fusion, 37* (1997).
[5] V.I. Vasiliev, Yu.A. Kostsov, K.M. Lobanov, L.P. Makarova, A.B. Mineev, V.K. Gusev, R.G. Levin, Yu.V. Petrov and N.V. Sakharov, *Nucl. Fusion 46*, 625 (2006).
[6] G.S. Kurskiev et al 2022 *Nucl. Fusion* 62 016011
[7] G.S. Kurskiev et al 2019 *Nucl. Fusion* 59 066032
[8] L.L. Lao et al 1985 *Nucl. Fusion* 25 1421

Corresponding author: erina.tkachenko@yandex.ru